Estimating primary production at depth from remote sensing

Z. P. Lee, K. L. Carder, J. Marra, R. G. Steward, and M. J. Perry

By use of a common primary-production model and identical photosynthetic parameters, four different methods were used to calculate quanta (Q) and primary production (P) at depth for a study of high-latitude North Atlantic waters. The differences among the four methods relate to the use of pigment information in the upper water column. Methods 1 and 2 use pigment biomass (B) as an input and a subtropical, empirical relation between K_d (diffuse attenuation coefficient) and B to estimate Q at depth. Method 1 uses measured B, but Method 2 uses B derived from the Coastal Zone Color Scanner (subtropical algorithm) as inputs. Methods 3 and 4 use the phytoplankton absorption coefficient (a_{ph}) instead of B as input, and Method 3 uses empirically derived $a_{\mathrm{ph}}(440)$ and K_d values, and Method 4 uses analytically derived $a_{\mathrm{ph}}(440)$ and a (total absorption coefficient) values based on the same remote measurements as Method 2. When the calculated and the measured values of $Q(z)$ and $P(z)$ were compared, Method 4 provided the closest results [for $P(z)$, $r^2 = 0.95$ ($n = 24$), and for $Q(z)$, $r^2 = 0.92$ ($n = 11$)]. Method 1 yielded the worst results [for $P(z)$, $r^2 = 0.56$ and for $Q(z)$, $r^2 = 0.81$]. These results indicate that one of the greatest uncertainties in the remote estimation of P can come from a potential mismatch of the pigment-specific absorption coefficient (a_{ph}^*), which is needed implicitly in current models or algorithms based on B. We point out that this potential mismatch can be avoided if we arrange the models or algorithms so that they are based on the pigment absorption coefficient (a_{ph}). Thus, except for the accuracy of the photosynthetic parameters and the above-surface light intensity, the accuracy of the remote estimation of P depends on how accurately a_{ph} can be estimated, but not how accurately B can be estimated. Also, methods to derive a_{ph} empirically and analytically from remotely sensed data are introduced. Curiously, combined application of subtropical algorithms for both B and K_d to subarctic waters apparently compensates to some extent for effects that are due to their similar and implicit pigment-specific absorption coefficients for the calculation of $Q(z)$.

Key words: Primary production, remote sensing, pigment absorption coefficients.

1. Introduction

Since the launch of the Coastal Zone Color Scanner (CZCS) in 1978, mapping primary production (P; symbols used in the text are summarized in Table 1) for the global ocean has been a goal for a number of researchers.[1–6] Because of the difficulty of estimating pigment biomass (B) from space, however, current methods can only account for $2/3$ of the variance in integral production.[6] Studies have been carried out to try to understand the variabilities[7–9] in P estimation, and it has been concluded that except for the variation of the photosynthetic parameters, the greatest uncertainty comes from the remotely derived pigment concentration.[5,6,10]

In this research, we suggest that at least for light-limited cases, one of the greatest uncertainties in remote estimation of P comes from a potential mismatch of the pigment-specific absorption coefficient (a_{ph}^*), which is needed explicitly or implicitly in current models or algorithms based on B. We also show that this potential mismatch can be avoided if we arrange the models or algorithms so that they are based on the phytoplankton absorption coefficient (a_{ph}). Thus, except for the accuracy of photosynthetic parameters and above-surface light intensity, the accuracy of remote estimation of P depends on

Z. P. Lee, K. L. Carder, and R. G. Steward are with the Department of Marine Science, University of South Florida, 140 7th Avenue North, St. Petersburg, Florida 33701. J. Marra is with the Lamont-Doherty Earth Observatory of Columbia University, Palisades, New York 10964. M. J. Perry is with the School of Oceanography, WB-10, University of Washington, Seattle, Washington 98195.

Received 15 May 1995; revised manuscript received 8 September 1995.

0003-6935/96/030463-12$06.00/0

Table 1. Symbols and Units

Symbol	Units	Description
a	m^{-1}	Total absorption coefficient, $a = a_w + a_{dg} + a_{ph}$
a_{dg}	m^{-1}	Absorption coefficient of detritus and gelbstoff
a_{ph}	m^{-1}	Absorption coefficient of phytoplankton pigments
a_{ph}^*	$m^2/(mg\ chl)$	Pigment-specific absorption coefficient
$\bar{a}_{ph}^*$	$m^2/(mg\ chl)$	Spectrally averaged a_{ph}^*
$a_{ph1,ph2}$	m^{-1}	$a_{ph}(440)$ and $a_{ph}(674)$, respectively
a_w	m^{-1}	Absorption coefficient of water molecules
A_1	mg/m^3	Parameter of the CZCS algorithm
A_2	—	Parameter of the CZCS algorithm
b_b	m^{-1}	Backscattering coefficient
B_{chl}	mg/m^3	Chlorophyll-a biomass
B	mg/m^3	Chlorophyll-a + pheophytin-a biomass
E_o	$Ein/m^2/nm$	Quantum scalar irradiance
K_d	m^{-1}	Diffuse attenuation coefficient for downwelling irradiance
K_w	m^{-1}	Diffuse attenuation coefficient for water molecules
K_ϕ	$Ein/m^2/day$	Value of Q where $\phi = \phi_m/2$
P	$mol\ C/m^3$	Primary production
Q	$Ein/m^2/day$	Photosynthetically available radiation (integrated from 400–700 nm)
R_{rs}	sr^{-1}	Remote-sensing reflectance
α	$mol\ C\ (mg\ chl)^{-1}\ (Ein\ m^{-2})^{-1}$	Rate of photosynthesis
α^B	$mol\ C\ (mg\ chl)^{-1}\ (Ein\ m^{-2})^{-1}$	Maximum rate of photosynthesis
ϕ	mol C/(Ein absorbed)	Quantum yield of photosynthesis
ϕ_m	mol C/(Ein absorbed)	Maximum quantum yield
λ	nm	Wavelength
$\mu_d(0)$	—	Subsurface average cosine for downwelling light field
ρ_1, ρ_2	—	Spectral ratio of remote-sensing reflectance
ν	$Ein/m^2/day$	Photoinhibition factor
χ	$m^2/(mg\ chl)$	Parameter for the empirical relation between K_d and B

how accurately a_{ph} can be estimated, but not on how accurately B can be estimated. Also, methods to derive a_{ph} empirically and analytically are introduced.

The pigment-specific absorption coefficient is often imbedded implicity in empirical algorithms for remote-sensing or in-water applications, or both. For example, the traditional pigment-concentration algorithm directly relates B to the ratio $L_w(443)/L_w(550) = \rho_{443,550}$ (L_w is the water-leaving radiance). As remote-sensing reflectance $R_{rs} = L_w/E_d$, and the phytoplankton absorption coefficient $a_{ph} = Ba_{ph}^*$, one may derive[11]

$$\rho_{443,550} \approx \frac{E_d(443)}{E_d(550)} \frac{b_b(443)}{b_b(550)} \times \frac{[a_w(550) + Ba_{ph}^*(550) + a_{dg}(550)]}{[a_w(443) + Ba_{ph}^*(443) + a_{dg}(443)]}, \quad (1)$$

where E_d is the downwelling irradiance above the surface, b_b is the backscattering coefficient, a_w is the absorption coefficient of water molecules, and a_{dg} is the absorption coefficient of detritus plus gelbstoff.

Thus, when $B \approx A_1[\rho_{443,550}]^{A2}$ results from regression analysis, the empirical values of A_1 and A_2 implicitly contain the behavior of $a_{ph}^*(\lambda)$ of the data set used to develop the algorithm. Similarly, when the diffuse attenuation coefficient K_d is expressed as $K_d = f(B)$, its empirical parameters implicitly include the a_{ph}^* values used in developing the empirical relation.[12]

If the environment in which the algorithms are applied is similar to those used in developing the empirical relation, the results should work reasonably well. If, for example, a subtropical data set was used to develop the regressions, and they are applied in a subarctic environment, a mismatch of a_{ph}^* may result. This helps to explain the factor-of-2–3 underestimation of chlorophyll concentration that results from the use of the CZCS pigment algorithm[13] for high-latitude waters.[14]

The same kind of argument can also be applied in the use of traditional primary-production models. Historically, as chlorophyll-a plays the central role in the process of photosynthesis and is ubiquitous in all photosynthetic systems, and variation of the amount of chlorophyll-a can account for much of the variation in observed primary production, perhaps also because of technique limitations, the concentration of chlorophyll-a (B_{chl}) or pigment (B) is more often measured than are their optical properties, and the concentration has been considered as an indicator of the effects of production. Traditionally, then, parameters involved in P models have been normalized to the concentration. Examples of this approach are shown in Eqs. (4a), (7a), and (8a) in Table 2. The logical result of such thinking was that if we can relate the quantity of interest to B, and derive B from remotely sensed data, then we can do the job remotely (one of the major reasons for the development of the CZCS algorithm[13] and other pigment-concentration algorithms[14]). However, when these models or algorithms are applied to the region of interest, it is hard to know *a priori* from space if we are using the right parameters without *in situ* measurements of α^B and a_{ph}^*. In most cases, we have to assume that the model parameters are consistent with those of the waters under study.

As discussed above, a recurring element in traditional approaches is the pigment-specific absorption coefficient. Specifically, parameters in Eqs. (4a),

Table 2. Mathematical Expressions Used for the *P* Calculation[a]

$$P(z) = \frac{K_\phi}{K_\phi + Q(z)}\,\mathrm{ftn}[\phi_m, \text{pigment}, E_0(\lambda, z)] \quad (2)$$

$$P(z) = \frac{K_\phi}{K_\phi + Q(z)}\,\mathrm{ftn}[\phi_m, \text{pigment}, E_0(\lambda, z)]\exp[-\nu Q(z)] \quad (3)$$

$$P(z) = \frac{K_\phi \exp[-\nu Q(z)]}{K_\phi + Q(z)} \int_\lambda \alpha^B(\lambda) B_{\mathrm{chl}} E_0(\lambda, z)\mathrm{d}\lambda \quad (4a)$$

$$P(z) = \frac{K_\phi \exp[-\nu Q(z)]}{K_\phi + Q(z)} \int_\lambda \phi_m a_{\mathrm{ph}}(\lambda) E_0(\lambda, z)\mathrm{d}\lambda \quad (4b)$$

$$Q(z) = \int_\lambda E_0(\lambda, z)\mathrm{d}\lambda \quad (5)$$

$$E_0(\lambda, z) \approx E_0(\lambda, 0)\exp[-1.08 K_d(\lambda) z] \quad (6)$$

$$K_d(\lambda) = K_w(\lambda) + \chi(\lambda) B^{e(\lambda)} \quad (7a)$$

$$K_d(\lambda) = M(\lambda)[K_d(490) - K_w(490)] + K_w(\lambda), \qquad K_d(490) = 0.19(\rho_2)^{-3.11}/\mu_d(0) \quad (7b)$$

$$B = A_1(\rho_1)^{A2} \quad (8a)$$

$$a_{\mathrm{ph}}(440) = 0.072(\rho_1)^{-1.62} \quad (8b)$$

[a] $\rho_1 = R_{\mathrm{rs}}(443)/R_{\mathrm{rs}}(550)$, $\rho_2 = R_{\mathrm{rs}}(520)/R_{\mathrm{rs}}(560)$. $K_w(\lambda)$ can be found in Morel,[12] Smith and Baker,[15] and Austin and Petzold[16]; $\chi(\lambda)$ and $e(\lambda)$ are found in Morel[12]; and $M(\lambda)$ are found in Austin and Petzold.[16] Relations between $K_d(490)$ and ρ_2 as well as between $a_{\mathrm{ph}}(440)$ and ρ_1 are from Lee.[17]

(7a), and (8a) are often developed independently, based on regression analysis, often from independent data sets. In fact, some of the parameters were developed based on lab data or field data from markedly different sites. In each development, if there was a dependency on pigment or chlorophyll-*a* concentration, the values of a_{ph}* were implicitly involved. Those values then were transferred to or imbedded in various parameters, such as α^B, χ, and A_1 in Table 2, with units related to pigment concentration. We know that if these empirical relations were not developed with the same database, they generally do not contain the same values of a_{ph}*. Thus, when we apply these parameters to sites of interest, it is difficult to know if they are consistent with each other or with the waters under study, or both, as pigment-specific absorption coefficients vary widely.[18–22] Also, values of a_{ph}* may be used implicitly two or three times [Eqs. (4a), (7a), and (8a)] in the process of calculating P. If two or perhaps three different a_{ph}* values are implicitly used, it is obvious that we cannot get accurate estimations of P even if we have accurate values regarding the photosynthetic parameters, the surface B, and the light intensity.

One way to avoid this uncertainty and to improve the model accuracy is explicit use of the same a_{ph}* for the whole process. However, for most of the current P models (production P–intensity I curves, for instance) and B algorithms (CZCS pigment-concentration algorithm, for instance), the values for a_{ph}* are not explicitly derived or available, but instead they are imbedded with other parameters in the empirical functionalities [α^B (photosynthetic rate) and A_1 in Table 2, for instance].

Another way to avoid a_{ph}* in the empirical parameters is by rearrangement of the production and the remote-estimation expressions for future remote-sensing applications [Eqs. (4b), (7b), and (8b) in Table 2, for instance]. In the rearranged expressions, a_{ph} will become the sole input regarding pigment in the water column [Eq. (4b)], and a_{ph} but not B is directly derived from remotely sensed data [Eq. (8b)], either analytically or empirically. Thus there is no involvement of a_{ph}* in the P calculation process. Alternatively, we can use the same representative a_{ph}* throughout the whole process when we know a_{ph} if we really want to show B in the expression, but it is obviously redundant for the purpose of estimating P.

In this paper, using a primary-production model, we evaluate four methods of parameterizing the photons absorbed and the diffuse attenuation coefficient for the calculation of P. The resulting P values are then compared with P measurements for six depths in the euphoric zone at four stations during a spring bloom south of Iceland.

2. Primary-Production Calculation

Mathematical expressions for the calculation of $P(z)$ based on remotely sensed data are summarized in Table 2. Here those expressions are developed.

For a well-mixed water column, primary production at depth can be expressed as[23–30]

$$P(z) = \phi(z) \int_\lambda a_{\mathrm{ph}}(\lambda) E_0(\lambda, z)\mathrm{d}\lambda. \quad (9)$$

In a mathematically equivalent form, Eq. (9) can be expressed as[10]

$$P(z) = \int_\lambda \alpha(\lambda, z) B_{\mathrm{chl}} E_0(\lambda, z)\mathrm{d}\lambda, \quad (10)$$

with

$$\alpha = \phi a_{\mathrm{ph}}^*,$$

where ϕ is the quantum yield of phytoplankton photosynthesis in mol C per Einsteins (Ein) absorbed (where 1 Ein = 6.02×10^{-23} quanta), α is the rate of photosynthesis in mol C mg chl $(\mathrm{Ein\ m^{-2}})^{-1}$, B_{chl} is the chlorophyll-*a* concentration in milligrams per cubic meter, and $E_0(\lambda, z)$ is the quantum scalar irradiance

at depth z in Ein m^{-2} nm^{-1}. The wavelength range of integration is 400–700 nm.

Modeling ϕ or α is beyond the scope of this study, and we use the same parameterization for all methods. Also, as Kiefer and Reynolds[31] indicated, ϕ is assumed to be independent of wavelength. Therefore, without loss of generality, the formula developed by Kiefer and Mitchell[30] is chosen for our applications. Then a general form for primary production at depth z is

$$P(z) = \frac{K_\phi}{K_\phi + Q(z)} \text{ftn}[\phi_m, \text{pigment}, E_0(\lambda, z)], \quad (2)$$

where function ftn represents the integral relation among photosynthesis, pigment, and quanta at depth z, with

$$Q(z) = \int_\lambda E_0(\lambda, z)d\lambda, \quad (5)$$

$$E_0(\lambda, z) \approx E_0(\lambda, 0)\exp[-1.08K_d(\lambda)z]. \quad (6)$$

The 1.08 above empirically accounts for the vertical average[32–34] of K_d, as K_d here stands for the subsurface value and $K_d \approx a/\mu_d(0)$. $\mu_d(0)$ is the subsurface average cosine for the downwelling light field.

In order to calculate P at depth with remote-sensing reflectance (R_{rs}) data, two more relations must be developed. First, to calculate light at depth [$E_0(\lambda, z)$], we need the diffuse attenuation coefficient [$K_d(\lambda)$]; second, we need a relation between in-water constituents and remotely measurable signals [Eqs. (8a) or (8b) in Table 2, for example].

As the chlorophyll concentration is traditionally considered as the index of the pigment in the water column, Eqs. (4a), (7a), and (8a) in Table 2, for instance, were developed. The calculation process is as follows: when the concentration is directly derived from remotely sensed data [Eq. (8a), $K_d(\lambda)$ can be calculated with Eq. (7a)]. Then $E_0(\lambda, z)$ and $Q(z)$ can be calculated with known $E_0(\lambda, 0)$; and finally, $P(z)$ can be estimated given $\alpha^B(\lambda)$ [Eq. (4a)]. With this approach, the focus of the method is on B, the pigment concentration. We refer to this approach below as being concentration based. In the calculation of P with this approach, parameters for A_1 and A_2 and for χ and e are taken from Gordon *et al.*[13] and Morel,[12] respectively.

Because of the wide variation of a_{ph}^* and the great uncertainty of predicting this parameter for a water environment, the A_1, A_2, χ, and e parameters may not be consistent with the waters under study. Therefore, Eqs. (4b), (7b), and (8b) in Table 2 were developed. As discussed above, the problem of specifying a_{ph}^* implicitly or explicitly is avoided with this approach. The parameters for Eqs. (7b) and (8b) were derived from Gulf of Mexico and Monterey Bay data,[17] with water types ranging widely from oligotrophic to riverine to coastal upwelling and B_{chl} values ranging from 0.07 to more than 40 mg/m^3.

The focus of this approach is to derive the absorption coefficient of the pigment and the diffuse attenuation coefficient of the water column directly, either empirically or analytically, from remotely sensed data. Below we refer to this type of approach as being absorption based. Here, as all functionalities are directly related to the absorption coefficient, no specific absorption coefficient is necessary. As a result, more consistent $P(z)$ and $Q(z)$ values should be expected relative to validation data sets.

Equations (4b), (7b), and (8b) in Table 2 provide examples of empirical methods to derive a_{ph} and K_d from remote-sensing reflectance data. Recently, a method to analytically derive a_{ph} and a from remotely measured hyperspectral data has been developed.[17,35] Results comparing the calculated Q and P for the concentration-based and the absorption-based approaches will ultimately be presented.

To show the differences and improvement in calculating $P(z)$ and $Q(z)$ from remotely sensed data by use of absorption-based approaches, the same daily $E_0(\lambda, 0)$ from measurements, and the same photosynthetic parameters (ϕ_m and K_ϕ) were used for the following four methods. For all calculations, the following parameters are used as needed[28,30,36]: ϕ_m = 0.06 mol C (Ein absorbed)$^{-1}$; K_ϕ = 10 Ein/day; and $\bar{a}_{ph}^*$ = 0.016 m^2 (mg Chl a)$^{-1}$, a spectral average used by many researchers.[26,37,38]

The spectral shape of $a_{ph}^*(\lambda)$ for the study area is shown in Fig. 1, which represents the cruise average. When pigment concentration is used as an input for the calculations, the ratio of B_{chl}/B is assumed to be equal to 0.8, a value based on the average in Balch *et al.*[6] In relating K_d and a, we use $\mu_d(0)$ = 0.83 for the high-latitude, cloudy days.[5,39]

Finally, for P calculations a photoinhibition parameter is applied, so Eq. (2) is adjusted to Eq. (3), and Eq. (3) is used for the four methods with ν = 0.01 [Ein/m^2/day]$^{-1}$, a value based on Platt *et al.*[40]

A. Method 1

With the measured B from the water column, $K_d(\lambda)$ is calculated with Eq. (7a), where values for $\chi(\lambda)$ and $e(\lambda)$ are from Morel.[12] Then $E_0(\lambda, z)$ is calculated with

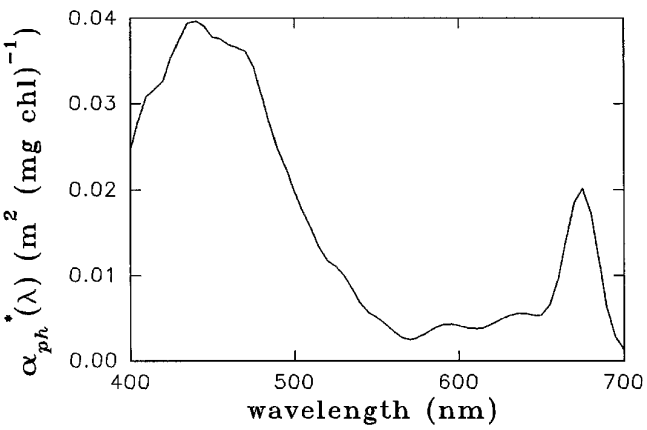

Fig. 1. $a_{ph}^*(\lambda)$ spectrum used in the study area.

Eq. (6). Therefore $P(z)$ and $Q(z)$ are calculated with Eqs. (4a) and (5), respectively.

B. Method 2

The same procedure as in Method 1 is used, except that B is derived with Eq. (8a) (the CZCS algorithm), which is adjusted for R_{rs} rather than L_w data. From Gordon *et al.*,[13] $A_1 = 1.13(0.95)^{-1.71} \approx 1.23$ and $A_2 = -1.71$, where 0.95 comes from $E_d(443)/E_d(550) \approx 0.95$.

C. Method 3

$K_d(490)$ and $a_{ph}(440)$ are derived with Eqs. (7b) and (8b), respectively, from the same measured R_{rs} curves. An empirical relation between $a(490)$ and R_{rs} was developed from our Gulf of Mexico and Monterey Bay data,[17] with a correlation coefficient $r^2 = 0.96$. Similar relations can be found in Austin and Petzold.[16] Expressions relating $K_d(\lambda)$ and $K_d(490)$ are from Austin and Petzold.[16]

The relation between $a_{ph}(440)$ and R_{rs} [Eq. (8b)] is developed for Gulf of Mexico waters ($r^2 = 0.87$) and is applied to the waters here as an example of using absorption by phytoplankton as a surrogate for pigment concentration, even though the environments are markedly different. Knowing $a_{ph}(440)$ from R_{rs} data, we then constructed $a_{ph}(\lambda)$ with a model suggested by Lee[17,35]:

$$a_{ph}(\lambda) = a_{ph1}\exp\left[-F\left(\ln\frac{\lambda-\lambda_1}{100}\right)^2\right], \quad 400 \le \lambda \le 570, \tag{11a}$$

$$a_{ph}(\lambda) = a_{ph}(570) + \frac{a_{ph}(656) - a_{ph}(570)}{656 - 570}(\lambda - 570), \quad 570 < \lambda < 656, \tag{11b}$$

$$a_{ph}(\lambda) = a_{ph2}\exp\left[-\frac{(\lambda-\lambda_2)^2}{2\sigma^2}\right], \quad 656 \le \lambda \le 700, \tag{11c}$$

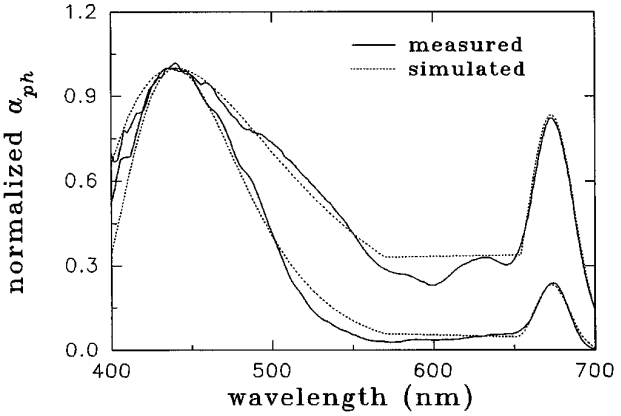

Fig. 2. Examples of $a_{ph}(\lambda)$ simulation (normalized at 440 nm, adapted from Lee[17]).

Table 3. Result Summary

Parameter	17 May	20 May	22 May	24 May
$Q(0)$ [Ein/m^2/day]	38.27	16.25	65.72	28.73
$R_{rs}(443)/R_{rs}(550)$	1.2	1.6	1.8	1.8
$R_{rs}(520)/R_{rs}(560)$	1.3	1.5	1.5	1.7
Surface B_{chl} (mg/m^3)	2.9	1.3	1.5	1.0
Surface B (mg/m^3)	3.6	1.6	1.9	1.3
CZCS B (mg/m^3)	0.89	0.57	0.47	0.43

with $a_{ph2}/a_{ph1} = 0.86 + 0.16\ln(a_{ph1})$, $F = 2.89\exp\{-0.505\tanh[0.56\ln(a_{ph1}/0.043)]\}$, and $\sigma = 14.17 + 0.9\ln(a_{ph1})$, where $a_{ph1} = a_{ph}(440)$, $a_{ph2} = a_{ph}(674)$, $\lambda_1 = 340$ nm, and $\lambda_2 = 674$ nm. The average difference between the measured and the simulated $a_{ph}(\lambda)$ if compared wavelength by wavelength is 11%.[17] However, the difference drops to approximately 2% when we compare the spectrally integrated $a_{ph}(\lambda)$ values (from 400 to 700 nm).[17] Figure 2 shows examples of measured versus simulated $a_{ph}(\lambda)$, which are normalized at 440 nm. This method can also be used with the CZCS, the Sea-Viewing Wide-field Sensor, or other data sets with limited spectral bands.

Knowledge of $a_{ph}(\lambda)$ and $K_d(\lambda)$ permits calculation of $P(z)$ and $Q(z)$ from Eqs. (4b) and (5), respectively.

D. Method 4

Given R_{rs} at N wavelengths, Lee[17] and Lee *et al.*[35,41] found

$$\begin{aligned} R_{rs}(\lambda_1) &\approx \frac{0.17}{a_w(\lambda_1) + a_{dg}(\lambda_1) + a_{ph}(\lambda_1)} \times \left[\frac{b_{bw}(\lambda_1)}{3.4} + X\left(\frac{400}{\lambda_1}\right)^Y\right], \\ &\vdots \\ R_{rs}(\lambda_N) &\approx \frac{0.17}{a_w(\lambda_N) + a_{dg}(\lambda_N) + a_{ph}(\lambda_N)} \times \left[\frac{b_{bw}(\lambda_N)}{3.4} + X\left(\frac{400}{\lambda_N}\right)^Y\right], \end{aligned} \tag{12}$$

where a_w and b_{bw} are the absorption and the backscattering coefficients of seawater, respectively, and can be found in Smith and Baker[15]; a_{dg} is the absorption coefficient of detritus and gelbstoff, and can be expressed as[19,42]

$$a_{dg}(\lambda) = a_{dg}(440)\exp[-S(\lambda - 440)]. \tag{13}$$

Table 4. Linear Analysis Results between Measured and Calculated $P(z)$ and $Q(z)$

	Method 1		Method 2		Method 3		Method 4	
Results	$P(z)$	$Q(z)$	$P(z)$	$Q(z)$	$P(z)$	$Q(z)$	$P(z)$	$Q(z)$
r^2	0.56	0.80	0.81	0.94	0.76	0.92	0.95	0.92
Error (ϵ)	1.57	1.18	0.87	0.27	0.38	0.28	0.25	0.18

X and Y describe the scattering effects of suspended particles.

Expressions (12) are a series of N expressions, which in total have at least $N + 4$ unknowns (N for a_{ph}, 2 for a_{dg}, and 2 for particle scattering) given only R_{rs}. However, when we use the $a_{ph}(\lambda)$ model [Eqs. (11)], the number of unknowns reduces to 5 [$a_{ph}(440)$, $a_{dg}(440)$, S, X and Y]. When the optimizing procedure developed by Lee[17] and Lee *et al.*[35] is used, the 5 unknowns can be solved, because N is >180 for our R_{rs} data. Thus $a_{ph}(\lambda)$ and $a(\lambda)$ (which is the sum of a_w, a_{dg}, and a_{ph}) can be derived for a wide range of environments and shapes of $a_{ph}(\lambda)$.

After the analytical retrieval of $a(\lambda)$ from measured R_{rs}, $K_d(\lambda)$ is derived with the relation $K_d(\lambda) \approx a(\lambda)/\mu_d(0)$, as $b_b \ll a$. Thus, with known $a_{ph}(\lambda)$ and $K_d(\lambda)$, P and Q values are calculated with Eqs. (4b) and (5), respectively.

3. Data and Measurements

Data on $Q(z)$, $P(z)$, and $R_{rs}(\lambda)$ were collected from 17 May to 24 May 1991 in the waters south of Iceland (21° W/ 59° N) on a Marine Light–Mixed Layer cruise. Q and P measurements were carried out with a floating array for 17, 20, 22, and 24 May. The sampling site, conditions, wind, mixing, and nutrients are presented in Marra *et al.*[43] and Pluedde-mann *et al.*[44] In general, it was windy throughout the cruise, and the euphotic zone was well mixed.

For *in situ* measurements, $Q(z)$ was monitored at four depths (0, 2, 12.5 and 25 m; no 2-m value was available for 22 May) and averaged for every 10-min interval throughout the day with Biospherical Q sensors attached to each incubation array.[43]

Dawn-to-dusk incubations (17 h) with four replicates were carried out *in situ* at each of six depths (5, 10, 15, 20, 30, and 40 m) chosen to span the euphotic zone. Primary-production measurements were made with the ^{14}C technique.[43]

Hyperspectral remote-sensing reflectance $R_{rs}(\lambda)$ was measured above the water from the ship by the use of the method developed by Carder and Steward[45] with the Spectron Engineering spectral radiometer (Model SE-590). The water-leaving radiance and the downwelling sky radiance were directly measured, and we measured downwelling irradiance by viewing a standard diffuse reflector (Spectralon, ~10% reflectance). Reflected sky radiance from the sea surface was corrected by the method of Carder and Steward[45] for calculation of $R_{rs}(\lambda)$.

4. Results and Discussion

Table 3 summarizes measured surface values for B_{chl} and Q, as well as the ratios of $R_{rs}(443)/R_{rs}(550)$ and

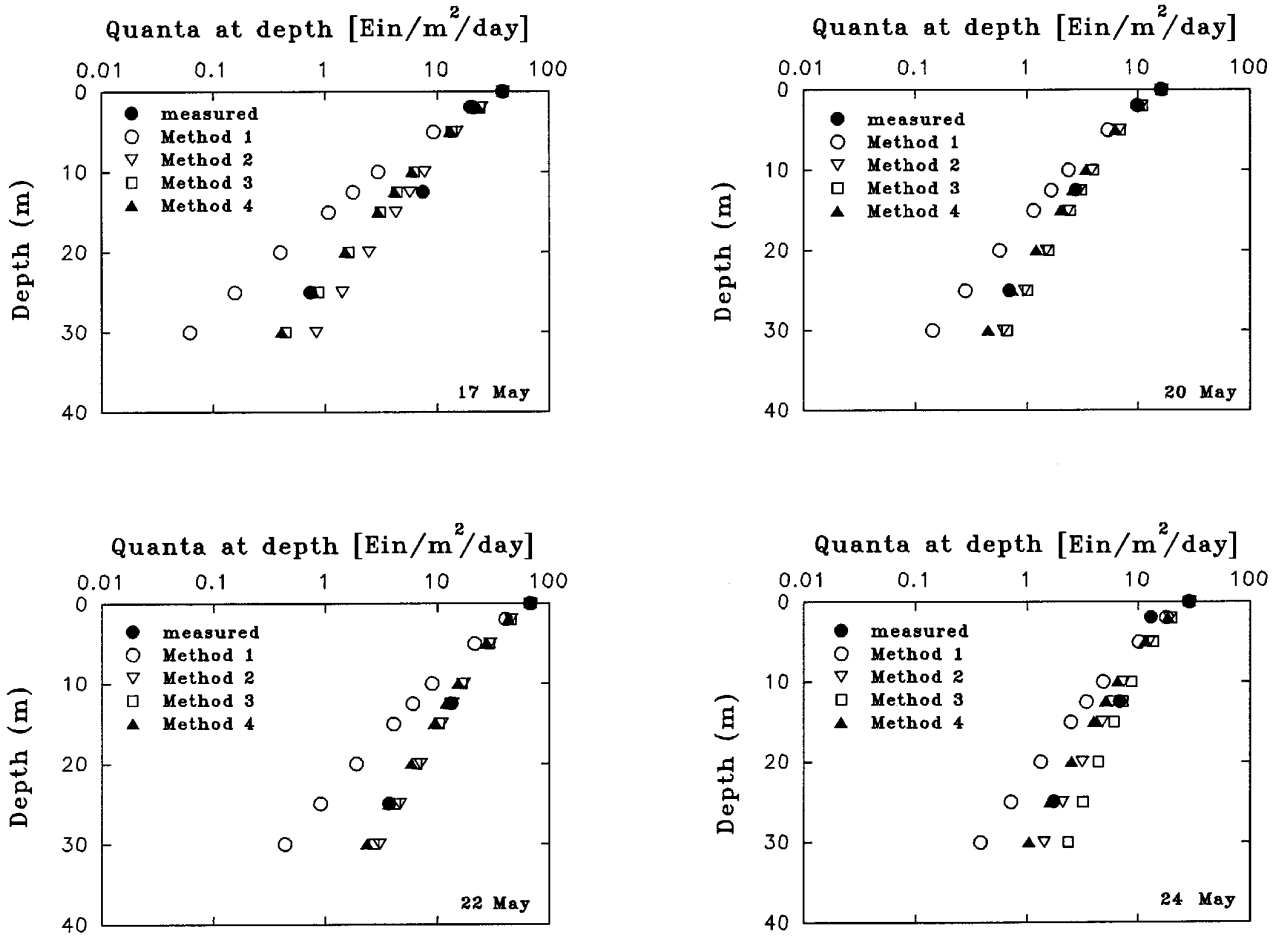

Fig. 3. Comparison of Q profiles for 17 May, 20 May, 22 May, and 24 May.

$R_{rs}(520)/R_{rs}(560)$. Pigment concentration (B) derived with the CZCS algorithm[13] is also presented.

Table 4 summarizes the results of the four methods, comparing the calculated and the measured P and Q values. Error (ϵ) in Table 4 is calculated as

$$\epsilon = \exp\left\{\mathrm{AVG}\left[\left|\ln\left(\frac{\mathrm{cal}}{\mathrm{mea}}\right)\right|\right]\right\} - 1. \quad (14)$$

where AVG means average. With a given ϵ, on average the measured value will fall in the range

$$\frac{\mathrm{cal}}{1+\epsilon} \le \mathrm{mea} \le (1+\epsilon)\mathrm{cal}. \quad (15)$$

This method of error calculation emphasizes that an equally large errors occur for underestimation and for overestimation. For example, errors are the same for cal/mea = 1/3 and for cal/mea = 3.0. However, traditional rms error is approximately 67% for cal/mea = 1/3 and 200% for cal/mea = 3.0.

Figures 3 and 4 compare station by station the measured and the calculated $Q(z)$ and $P(z)$ vertical profiles, respectively. In comparing the four methods, in Fig. 5 we show the measured and the calculated $Q(z)$ for the 4 measurement days, except for the surface values, and Fig. 6 shows the measured and the calculated $P(z)$ for the 4 days. Linear analyses were performed for the data in Figs. 5 and 6, and the results are presented in Table 4.

A. Surface B

B values estimated with the CZCS algorithm are as much as a factor of 4 lower than the measured surface values for these waters. This difference very likely indicates that there was a mismatch between the a_{ph}* in the CZCS algorithm and a_{ph}* for this high-latitude water environment,[14,46] or (less likely) that there were substantial errors or discrepancies in the measurements of R_{rs} or pigment-concentration values. Similar comparisons for subtropical waters have typically been within approximately a factor of 2 over measured values.[13]

B. $Q(z)$

Method 1 provided the worst results at depth, with calculated values as much as 2.18 times smaller than measured data (error $\epsilon = 1.18$). This might be because of the fact that Eq. (7a) was developed with largely temperate and subtropical data sets,[12] where the specific absorption coefficients are likely to be much higher than those of the waters of this study. The improper use of high pigment-specific absorption coefficients with measured B values would cause

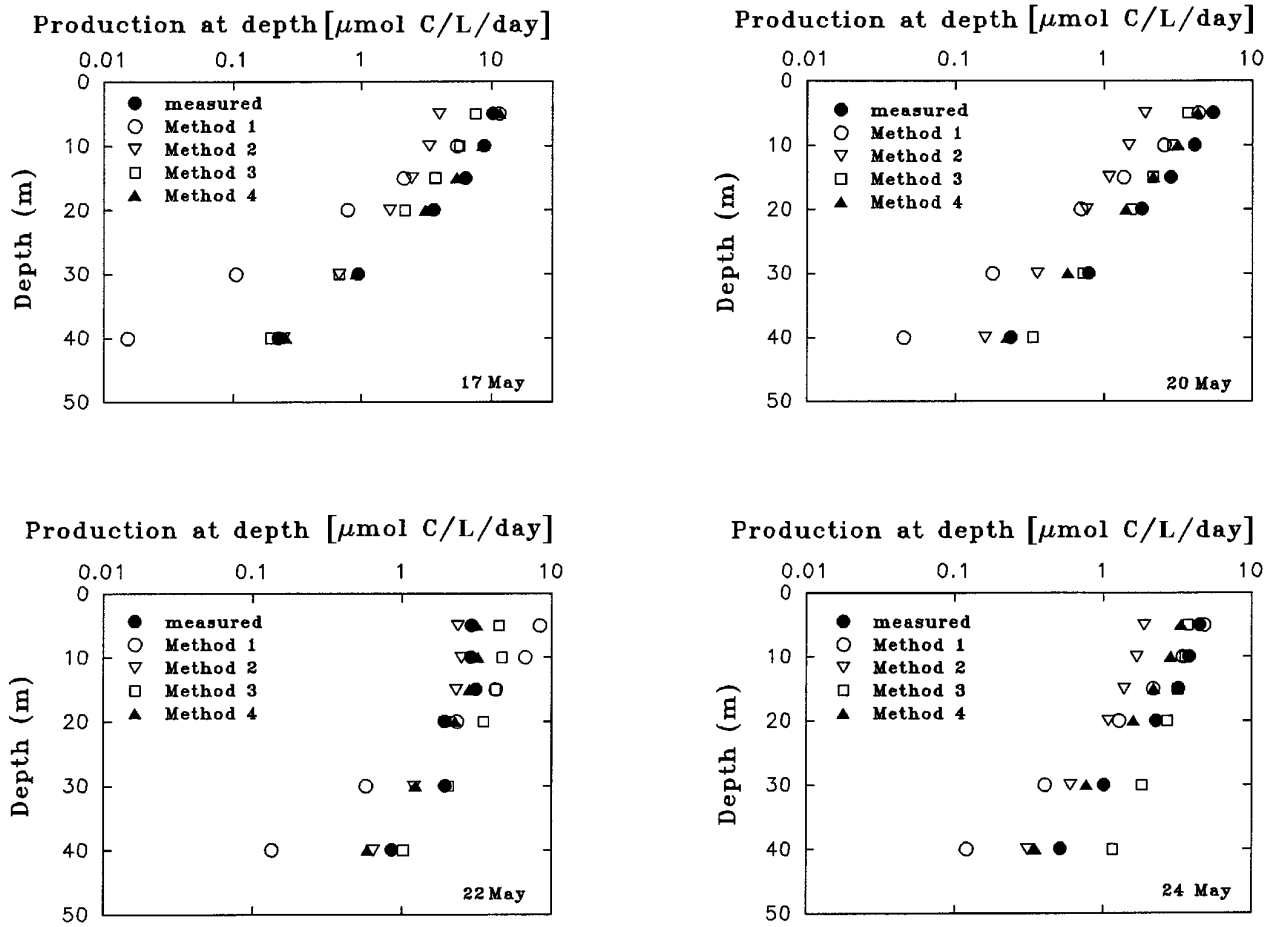

Fig. 4. Comparison of P profiles for 17 May, 20 May, 22 May, and 24 May. L, liter.

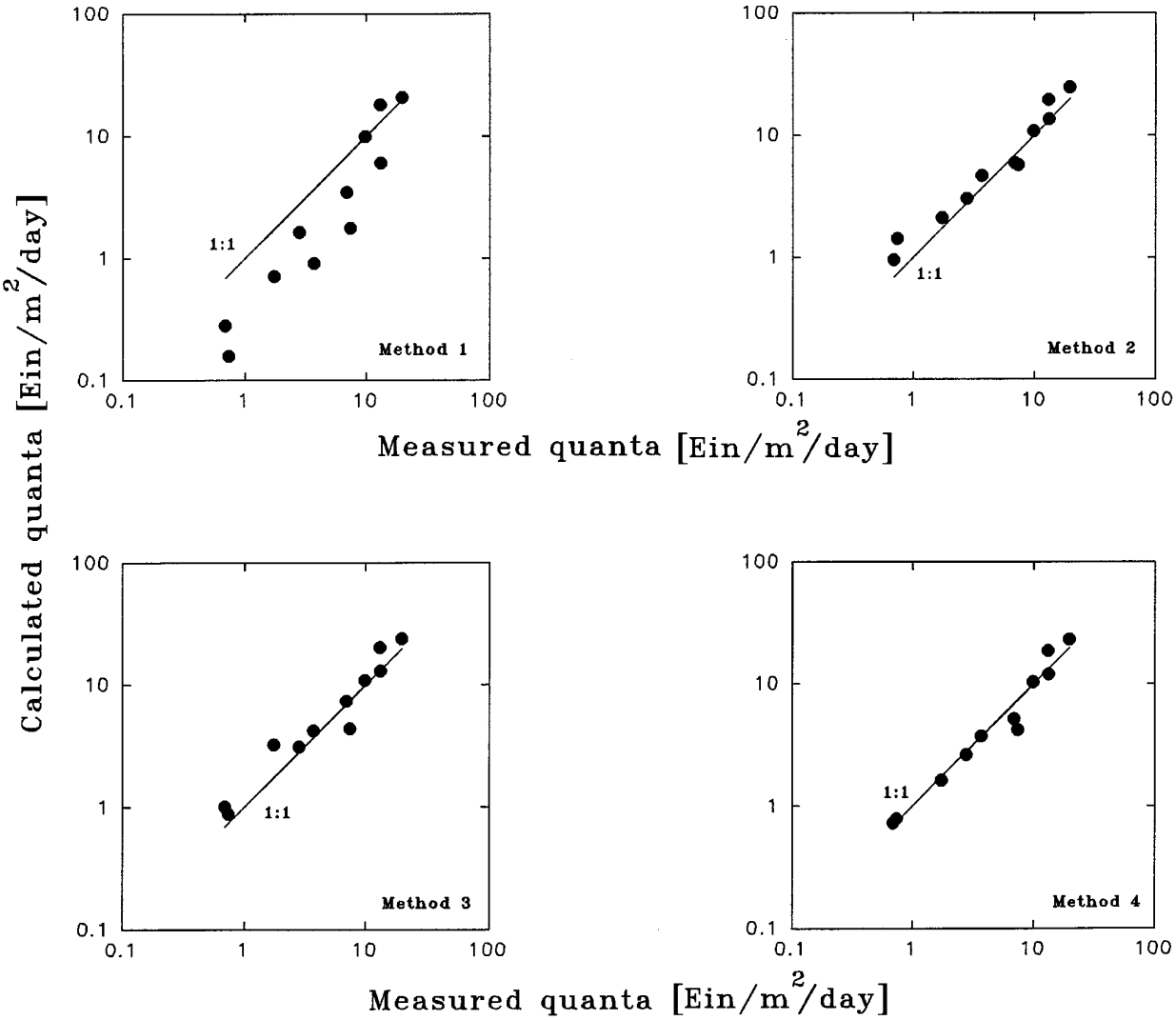

Fig. 5. Comparison among the measured and the calculated $Q(z)$ of the 4 measurement days (no surface values) among the four methods.

calculated K_d values to be high and thus cause Q to be low at depth. These low Q values might also cause P to be low at depth. These results indicate that when there is a mismatch between the region studied and the region in which an empirical model was developed, the specific absorption coefficient is likely to be different for the two regions. Then further applications of an empirical bio-optical model can go awry even when we have measured biomass.

Method 2 resulted in much more accurate $Q(z)$ values, with calculated values averaging approximately 1.27 times the measured ones (error $\epsilon = 0.27$). This seems amazing considering that the CZCS-derived B values are a factor of 4 lower than the measured ones. That this is possible is likely due to the fact that both Eqs. (7a) and (8a) were developed from mostly tropical or subtropical or summer temperate data sets. This suggests that similar specific absorption coefficients were imbedded in both Eqs. (7a) and (8a). So an error in B when Eq. (8a) is used is compensated for when Eq. (7a) is used to calculate K_d. Actually, when $K_d(490)$ and the R_{rs} ratio ρ_1 $[= R_{rs}(443)/R_{rs}(550)]$ are directly related, a combination of Eqs. (7a) and (8a) provides $K_d(490) \approx K_w(490) + 0.080(\rho_1)^{-1.20}$, which is not far from the empirical relation developed by Austin and Petzold.[16] So, for the estimation of K_d or $Q(z)$, or both, the combination of Eqs. (7a) and (8a) may be used in concert for a much wider range of environments, up to and including high-latitude waters, than either of the individual equations, although they were developed based on data from tropical or subtropical environments.

Method 3 provided similar results to Method 2, which means that Eq. (8b) can be used widely, although it was developed with markedly different water environments. The reason for this is, in part, that no specific absorption coefficients are involved in this application, reducing the odds that a mismatch of specific absorption coefficients might occur.

Method 4, as expected, yielded the lowest error ($\epsilon = 0.18$), because the parameters are analytically derived with hyperspectral data rather than being dependent on empirical relations that use only a few

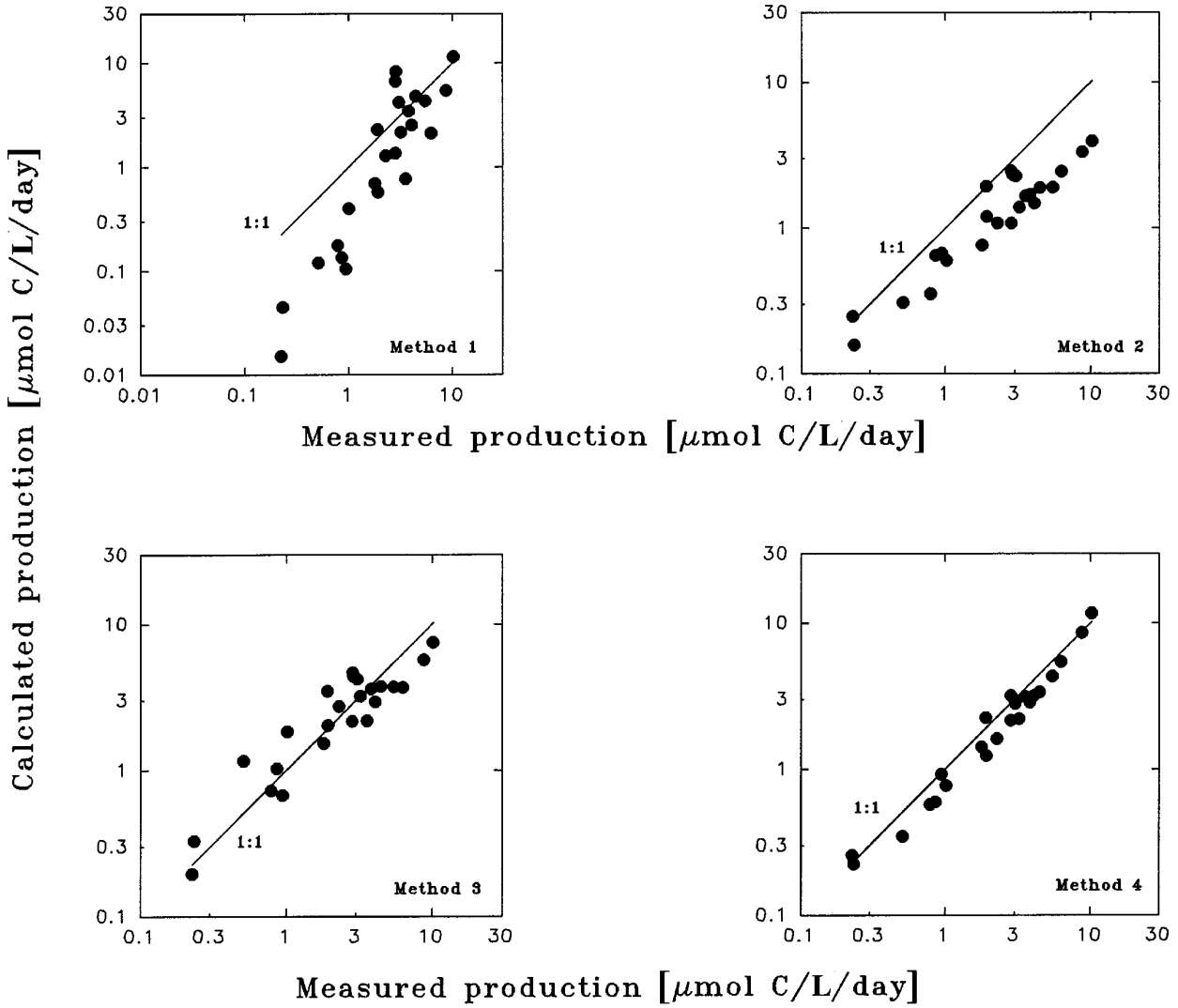

Fig. 6. Comparison among the measured and the calculated $P(z)$ of the 4 measurement days among the four methods.

channels, with no dependence on specific absorption coefficients.

C. $P(z)$

Although measured pigment concentrations were used, Method 1 did not provide good estimates for either Q or P, probably because of a high, implicit specific absorption coefficient in the bio-optical relation [Eq. (7a)] but a correct photosynthetic parameter (α^B) in the bioproduction relation [Eq. (4a)]. The P values calculated by use of Method 1 were on average 2.57 times smaller than the measured ones (error $\epsilon = 1.57$).

At the surface, P values calculated with Method 2 were nearly a factor of 3 lower than the measured rates, even though the Q values that were calculated aproximated those that were measured. This might be the result of a low biomass number being multiplied by a correct specific absorption coefficient (or α^B), resulting in a reduction in the calculated quanta absorbed by phytoplankton for Method 2. This is consistent with the conclusion of Platt *et al.*[5,10] that determination of biomass with remote sensing dominates the error in primary-production estimations.

The absorption methods, however, resulted in much-improved performances. Method 3, which is also empirical and uses the same R_{rs} ratio, provided an improved estimation of $P(z)$, where the error (ϵ) is reduced to approximately half that for Method 2 when the same photosynthetic parameters are used. Method 4 ultimately resulted in the lowest error, not only for $Q(z)$ ($\epsilon = 0.18$), but also for $P(z)$ ($\epsilon = 0.25$). This means that Methods 3 and 4 work fine for the waters studied, even though the $a_{ph}(\lambda)$ model and $a_{ph}(440)$ algorithm were developed with the Gulf of Mexico data[17] and the $P(z)$ model was developed with laboratory data.[30]

It should be pointed out that a reduction in error (ϵ) by a factor of 3 for P for Method 4 compared with Method 2 does not mean that Method 4 improves the accuracy of calculation of $P(z)$ by that factor. The reason for this is that the value of ϵ is also dependent on the photosynthetic parameters (ϕ_m, K_ϕ, and ν). For example, if we double ϕ_m, ϵ for both methods will

be approximately the same; if we triple ϕ_m, ϵ for Method 2 will be lower than that for Method 4. The theoretical maximum[26] for ϕ_m, however, is approximately 0.12 mol C (Ein absorbed)$^{-1}$, and most of the reported ϕ_m values[47–49] fall in the range of 0.04–0.08 mol C (Ein absorbed)$^{-1}$. Thus the 0.06 mol C (Ein absorbed)$^{-1}$ values used here for ϕ_m is quite representative of expected values for this region.[28,34,43]

Most of the error for Method 2 in calculating $P(z)$ apparently comes from the mismatch of the pigment-specific absorption coefficients implicitly used in Eqs. (4a) and (8a). If we believe the value for α^B (the product of ϕ_m and a_{ph}*) is reasonable, however, then the pigment derived with Eq. (8a) must cause most of the error in $P(z)$. Thus regional and seasonal pigment algorithms have to be developed in order to correct or compensate for the possible mismatch of a_{ph}* between the bioproduction and the bio-optical expressions if models such as Method 2 are to be used effectively.

Because there is no dependence of P on a_{ph}* when the absorption-based approach is used [Eqs. (4b), (7b), and (8b) in Table 2], there is no need for regionally or seasonally adjusted pigment-concentration algorithms, and we do not need to know the pigment concentration for $P(z)$ estimation from remote-sensing data. However, to use the empirical absorption method, site-specific adjustments to the parameters might be required for Eq. (8b) to be used for various environments, because a single spectral ratio cannot adequately separate the absorption effects of pigments from those due to gelbstoff and detritus.

For the photosynthetic parameters, α^B can vary by a factor of 4 for the same season for different regions, a factor of 4 for the same region for different seasons, or a factor of 5 for different regions and seasons.[5] This may, in large part, be the result of variations of a_{ph}*, which are imbedded in α^B. Although ϕ_m = 0.06 mol C (Ein absorbed)$^{-1}$ worked quite well for our situation, we certainly want to know the range for ϕ_m under a wider variety of conditions. If we can predict ϕ_m with reasonable accuracy for different regions or seasons, or both, the accuracy in estimating $P(z)$ will be further improved for the global ocean.

For the three photosynthetic parameters, values of K_ϕ and ν have more influence on P value at the surface than at depth, and ϕ_m has the same weight all over the depth. Only when $Q(z)$ is very high is ν a significant factor in P calculations. For example, for $\nu = 0.01$ (Ein/m^2/day)$^{-1}$, $\exp[-\nu Q(z)]$ is 0.90, 0.82, 0.67, 0.55, and 0.45 for $Q(z)$ values of 10, 20, 40, 60, and 80 (Ein/m^2)/day, respectively. This means that when the photoinhibition term is dropped, the calculated P value will increase by 10% to 55% accordingly. Without the photoinhibition term, however, the possible increase and then decrease in the vertical structure of P with depth would not be simulated.

5. Conclusions and Expectations

(1) It is not necessary to know B for the calculation of P with remote-sensing methods. What is more important for the calculation of P is the absorption by the phytoplankton pigments, the attenuation of the water column, and the photosynthetic parameters of phytoplankton in the water column.

(2) The Q and P values calculated by the use of the absorption-based approaches approximated the measured values. This indicates that the optical parameters in the P calculation can be quite accurately estimated from remotely sensed data, especially when the hyperspectral, analytical approach (Method 4) is used. The empirical absorption approach (Method 3) was slightly less accurate.

(3) It appears that improved maps of the global P with the existing CZCS data might be made with Method 3.

(4) Investigations focusing on accurately deriving a_{ph} and a from remote-sensing measurements need to be carried out widely, and more data sets including K_d, Q, a_{ph}, a, P, and R_{rs} are needed to test and improve the absorption-based approach.

(5) For the estimation of P with remote-sensing data, methods must be pursued to estimate the photosynthetic parameters, perhaps by their covariance with some remotely measured variables such as sea-surface temperature anomalies, wind-stress history, chlorophyll fluorescence, and light history.

The authors thank the Captain and crew of the R/V Endeavor for their help and their professionalism on the Marine Light–Mixed Layer cruise. The comments and suggestions made by Shubha Sathenydranath and Gabriel Vargo are greatly appreciated. This research was supported by U.S. Office of Naval Research (ONR) grants N00014-89-J-1091, and N00014-94-L-0114 and NASA grant NAGW-465 to the University of South Florida.

References

1. R. C. Smith, R. W. Eppley, and K. S. Baker, "Correlation of primary production as measured aboard ship in Southern California Coastal waters and as estimated from satellite chlorophyll images," Mar. Biol. **66,** 281–288 (1982).
2. R. W. Eppley, E. Stewart, M. R. Abbott, and U. Heyman, "Estimating ocean primary production from satellite chlorophyll: introduction to regional differences and statistics for the Southern California Bight," J. Plankton Res. **7,** 57–70 (1985).
3. A. Morel, "Light and marine photosynthesis: a spectral model with geochemical and climatological implications," Prog. Oceanogr. **26,** 263–306 (1991).
4. A. Morel and J.-M. Andre, "Pigment distribution and primary production in the Western Mediterranean as derived and modeled from Coastal Zone Color Scanner observations," J. Geophys. Res. **96,** 12685–12698 (1991).
5. T. Platt, C. M. Caverhill, and S. Sathyendranath, "Basin-scale estimates of oceanic primary production by remote sensing: the North Atlantic," J. Geophys. Res. **96,** 15147–15159 (1991).
6. W. M. Balch, R. Evans, J. Brown, G. Feldman, C. McClain, and W. Esaias, "The remote sensing of ocean primary productivity: use of a new data compilation to test satellite algorithms," J. Geophys. Res. **97,** 2279–2293 (1992).
7. S. Sathyendranath, T. Platt, C. M. Caverhill, R. E. Warnock, and M. R. Lewis, "Remote sensing of oceanic primary production: computations using a spectral model," Deep-Sea Res. **36,** 431–453 (1989).

8. A. Morel and J. F. Berton, "Surface pigments, algal biomass profiles, and potential production of the euphotic layer: relationships reinvestigated in review of remote-sensing applications," Limnol. Oceanogr. **34,** 1545–1562 (1989).
9. K. Banse and M. Yong, "Sources of variability in satellite-derived estimates of phytoplankton production in the Eastern Tropical Pacific," J. Geophys. Res. **95,** 7201–7215 (1990).
10. T. Platt, S. Sathyendranath, C. M. Caverhill, and M. R. Lewis, "Ocean primary production and available light: further algorithms for remote sensing," Deep-Sea Res. **35,** 855–879 (1988).
11. H. R. Gordon and A. Morel, *Remote Assessment of Ocean Color for Interpretation of Satellite Visible Imagery: A Review* (Springer-Verlag, New York, 1983).
12. A. Morel, "Optical modeling of the upper ocean in relation to its biogenous matter content (case I waters)," J. Geophys. Res. **93,** 10749–10768 (1988).
13. H. R. Gordon, D. K. Clark, J. W. Brown, O. B. Brown, R. H. Evans, and W. W. Broenkow, "Phytoplankton pigment concentrations in the Middle Atlantic Bight: comparison of ship determinations and CZCS estimates," Appl. Opt. **22,** 20–36 (1983).
14. B. G. Mitchell and O. Holm-Hansen, "Bio-optical properties of Antarctic Peninsula waters: differentiation from temperate ocean models," Deep-Sea Res. **38,** 1009–1028 (1991).
15. R. C. Smith and K. S. Baker, "Optical properties of the clearest natural waters," Appl. Opt. **20,** 177–184 (1981).
16. R. W. Austin and T. J. Petzold, "Spectral dependence of the diffuse attenuation coefficient of light in ocean waters," in *Ocean Optics VII,* M. A. Blizard, ed., Proc. Soc. Photo-Opt. Instrum. Eng. **489,** 168–178 (1984).
17. Z. P. Lee, "Visible-infrared remote-sensing model and applications for ocean waters," Ph.D. dissertation (University of South Florida, St. Petersburg, 1994), Dissertation Abstract International 56-01B (UMI Microfilm, Ann Arbor, Mich., 1995).
18. A. Morel and A. Bricaud, "Theoretical results concerning light absorption in a discrete medium and application to the specific absorption of phytoplankton," Deep-Sea Res. **28,** 1357–1393 (1981).
19. M. Kishino, N. Okami, M. Takahashi, and S. Ichimura, "Light utilization efficiency and quantum yield of phytoplankton in a thermally stratified sea," Limnol. Oceanogr. **31,** 557–566 (1986).
20. A. Bricaud, A.-L. Bedhomme, and A. Morel, "Optical properties of diverse phytoplanktonic species: experimental results and theoretical interpretation," J. Plankton Res. **10,** 851–873 (1988).
21. E. A. Laws, G. R. Ditullio, K. L. Carder, P. R. Betzer, and S. K. Hawes, "Primary production in the deep blue sea," Deep-Sea Res. **37,** 715–730 (1990).
22. K. L. Carder, S. K. Hawes, K. S. Baker, R. C. Smith, R. G. Steward, and B. G. Mitchell, "Reflectance model for quantifying chlorophyll *a* in the presence of productivity degradation products," J. Geophys. Res. **96,** 20599–20611 (1991).
23. J. T. O. Kirk, *Light and Photosynthesis in Aquatic Ecosystems* (Cambridge U. Press, London, 1986), p. 239.
24. R. R. Bidigare, R. C. Smith, K. S. Baker, and J. Marra, "Oceanic primary production estimates from measurements of spectral irradiance and pigment concentrations," Global Biogeochemical Cycles **1,** 171–186 (1987).
25. R. R. Bidigare, B. B. Prezelin, and R. C. Smith, "Bio-optical models and the problems of scaling," in *Primary Production and Biogeochemical Cycles in the Sea,* P. G. Falkowski and A. D. Woodhead, eds. (Plenum, New York, 1992), pp. 175–212.
26. R. C. Smith, B. B. Prezelin, R. R. Bidigare, and K. S. Baker, "Bio-optical modeling of photosynthetic production in coastal waters," Limnol. Oceanogr. **34,** 1524–1544 (1989).
27. J. J. Cullen, "On models of growth and photosynthesis in phytoplankton," Deep-Sea Res. **37,** 667–683 (1990).
28. J. Marra, T. Dickey, W. S. Chamberlin, C. Ho, T. Granata, D. A. Kiefer, C. Langdon, R. C. Smith, K. S. Baker, R. R. Bidigare, and M. Hamilton, "Estimation of seasonal primary production from moored optical sensors in the Sargasso Sea," J. Geophys. Res. **97,** 7399–7412 (1992).
29. J. R. V. Zaneveld, J. C. Kitchen, and J. L. Mueller, "Vertical structure of productivity and its vertical integration as derived from remotely sensed observations," Limnol. Oceanogr. **38,** 1384–1393 (1993).
30. D. A. Kiefer and B. G. Mitchell, "A simple, steady state description of phytoplankton growth based on absorption cross section and quantum efficiency," Limnol. Oceanogr. **28,** 770–776 (1983).
31. D. A. Kiefer and R. A. Reynolds, "Advances in understanding phytoplankton fluorescence and photosynthesis," in *Primary Production and Biogeochemical Cycles in the Sea,* P. G. Falkowski and A. D. Woodhead, eds. (Plenum, New York, 1992), pp. 155–174.
32. H. R. Gordon, "Can the Lambert-Beer law be applied to the diffuse attenuation coefficient of ocean water?" Limnol. Oceanogr. **34,** 1389–1409 (1989).
33. T. T. Bannister, "Model of the mean cosine of underwater radiance and estimation of underwater scalar irradiance," Limnol. Oceanogr. **37,** 773–780 (1992).
34. K. L. Carder, Z. P. Lee, J. Marra, R. G. Steward, and M. J. Perry, "Calculated quantum yield of photosynthesis of phytoplankton in the Marine Light–Mixed Layers (50 °N/21 °W)," J. Geophys. Res. **100,** 6655–6663 (1995).
35. Z. P. Lee, K. L. Carder, T. G. Peacock, C. O. Davis, and J. Mueller, "Method to derive ocean absorption coefficients from remote-sensing reflectance," Appl. Opt. **35,** 453–462 (1996).
36. J. Marra, W. S. Chamberlin, and C. A. Knudson, "Proportionality between in situ carbon assimilation and bio-optical measures of primary production in the Gulf of Maine in summer," Limnol. Oceanogr. **38,** 232–238 (1993).
37. T. T. Bannister, "Production equations in terms of chlorophyll concentration, quantum yield, and upper limit to production," Limnol. Oceanogr. **19,** 1–12 (1974).
38. Z. Dubinsky, T. Berman, and F. Schanz, "Field experiments for *in situ* measurements of photosynthetic efficiency and quantum yield," J. Plankton Res. **6,** 339–349 (1984).
39. S. Sathyendranath and T. Platt, "The spectral irradiance field at the surface and in the interior of the ocean: a model for applications in oceanography and remote sensing," J. Geophys. Res. **93,** 9270–9280 (1988).
40. T. Platt, C. L. Gallegos, and W. G. Harrison, "Photoinhibition of photosynthesis in natural assemblages of marine phytoplankton," J. Marine Res. **38,** 687–701 (1980).
41. Z. P. Lee, K. L. Carder, S. K. Hawes, R. G. Steward, T. G. Peacock, and C. O. Davis, "A model for interpretation of hyperspectral remote sensing reflectance," Appl. Opt. **33,** 5721–5732 (1994).
42. C. S. Roesler, M. J. Perry, and K. L. Carder, "Modeling in situ phytoplankton absorption from total absorption spectra in productive inland marine waters," Limnol. Oceanogr. **34,** 1510–1523 (1989).
43. J. Marra, C. Langdon, and C. A. Knudson, "Primary production and water column changes and the demise of a *phaeocystis* bloom at the Marine Light–Mixed Layers site (59 °N/21 °W, North Atlantic Ocean)," J. Geophys. Res. **100,** 6521–6526 (1995).
44. A. Plueddemann, R. Weller, T. Dickey, J. Marra, and M. Stramska, "Surface forcing and re-stratification in the sub-Arctic North Atlantic," J. Geophys. Res. **100,** 6605–6620 (1995).

45. K. L. Carder and R. G. Steward, "A remote-sensing reflectance model of a red tide dinoflagellate off West Florida," Limnol. Oceanogr. **30,** 286–298 (1985).
46. W. M. Balch, R. W. Epply, M. R. Abbott, and F. M. H. Reid, "Bias in satellite-derived pigment measurements due to coccolithophores and dinoflagellates," J. Plankton Res. **11,** 575–581 (1989).
47. C. Langdon, "On the causes of interspecific differences in growth–irradiance relationship for phytoplankton. II. A general review," J. Plankton Res. **10,** 1291–1312 (1988).
48. J. S. Cleveland, M. J. Perry, D. A. Kiefer, and M. C. Talbot, "Maximal quantum yield of photosynthesis in the Northwestern Sargasso Sea," J. Mar. Res. **47,** 869–886 (1989).
49. T. T. Bannister and A. D. Weidemann, "The maximum quantum yield of phytoplankton photosynthesis *in situ,*" J. Plankton. Res. **6,** 275–294 (1984).